Optics and Photonics Journal, 2025, 15(2), 9-20
https://www.scirp.org/journal/opj
ISSN Online: 2160-889X
ISSN Print: 2160-8881

Simulation of Some Optical Phenomena Observed in the Chadian Atmosphere

Foulla Dieudonné Platou[1,2*], Abdallah Brahim Elhadj Ali[3], Zoutchibé Joseph[1,4], Bakesseng Konwondi Freud[1], Mahamat Barka[1]

[1]Department of Physics, Faculty of Exact and Applied Science, University of N'Djamena, N'Djamena, Chad
[2]Laboratory of Photonics, Department of Physics, Faculty of Science, University of Ngaoundere, Ngaoundere, Cameroon
[3]Centre National de Recherche pour le Développement, N'Djamena, Tchad
[4]Laboratoire Optique et Applications, Centre of Atomic Molecular Physics and Quantum Optics, Faculty of Sciences, University of Douala, Douala, Cameroon
Email: *foulladieudo@gmail.com

How to cite this paper: Platou, F.D., Ali, A.B.E., Joseph, Z., Freud, B.K. and Barka, M. (2025) Simulation of Some Optical Phenomena Observed in the Chadian Atmosphere. *Optics and Photonics Journal*, **15**, 9-20.
https://doi.org/10.4236/opj.2025.152002

Received: January 20, 2025
Accepted: February 25, 2025
Published: February 28, 2025

Abstract

This research focuses on simulating mirages, rainbows, and halos in the atmosphere of Chad. Simulation of the refractive index with temperature shows that the city of Moundou in the tropical climate and those of N'Djamena, Mongo, and Abeche in the Sahelian climate experience a strong alternation of superior and inferior mirages throughout the year. In contrast, in Faya-Largeau, which has a desert climate, both phenomena are observed throughout the year. The presence of abundant and moderate rainfall, respectively in Moundou in the tropical climate, and in Abeche, Mongo, and N'Djamena in the Sahelian climate, could give rise to the observation of rainbows. However, the absence of rainfall in the desert climate makes it almost impossible to observe rainbows in the city of Faya-Largeau.

Keywords

Inferior Mirage, Superior Mirage, Refraction Index, Halos, Simulation

1. Introduction

In the atmosphere, the propagation of light from one point to another undergoes the phenomenon of refraction [1] [2]. Atmospheric refraction is a phenomenon that consists of a non-straight trajectory of light as it passes from one medium to another [2] [3]. In fact, this change in the direction of light as it passes through is due to the fact that the refractive index of light is not constant in the space through which it propagates. The refractive index depends on the humidity and density of the air, which in turn depends on the temperature and pressure at different altitudes in the atmosphere [4].

Historically, the first approach to the law of refraction was undertaken by Ptolemy in the 11th century, who created a table correlating the angles of incidence and refraction of light for air/water, air/glass, and water/glass interfaces [5]. These different values seemed to obey a law, but Ptolemy did not translate them into a mathematical formula, so that the correspondences with the actual values remained quite approximate. It was in 1637 that René Descartes published this law of refraction in his famous work Dioptrics [5]. For objects immersed in the atmosphere, we refer to terrestrial refraction for an observer located on the ground, which leads to the phenomenon of mirages [6] [7]. Mirages are an optical phenomenon resulting from the refraction of light caused by differences in refractive indices. [7]. These differences are often due to temperature variations that alter air density. Light bends as it passes through layers of air of different densities, creating an optical illusion. Depending on the position of the image perceived by the observer, either a superior mirage or an inferior mirage is observed. An inferior mirage occurs over large, flat, sunny surfaces, where the air near the ground is warmer than the air just above it [8] [9]. If, on the other hand, the air at ground level is colder than the air above, a superior mirage is observed [10] [11]. In the atmosphere, these optical phenomena occur in the case of strong temperature inversions.

When light enters a prism of clouds at varying temperatures, the refractive index also varies, causing the light to disperse as it exits the prism of clouds. This is the rainbow phenomenon commonly observed in the sky. Rainbows are an optical and meteorological phenomenon that makes the continuous spectrum of light in the sky visible when the sun shines while it is raining. They are directly linked to precipitation, as they are formed by the refraction of light on raindrops (precipitation), which breaks down white light into its different spectra, or colors, and the reflection behind the plane that makes these different rainbow colors visible. A rainbow contains as many colors as can be distinguished, up to a maximum of 150 [6]. First, light is refracted as it enters the surface of the raindrop, then it undergoes partial reflection back from the same raindrop. Another optical phenomenon observable in the atmosphere is halos. Halos result from the interaction between ice crystals and a light beam propagating through the space in question. A halo is formed when the sky is clear, with light cloud cover at high altitude. The clouds that contribute to halo formation are cirrus clouds at altitudes of between 5000 and 10,000 meters [12]. It is formed by vaporous, diffuse clouds in a fairly cold atmosphere, allowing water vapors to solidify in crystalline, hexagonal form.

The study of the refractive index of the atmosphere in Madagascar, more precisely, of the capital ANTANANARIVO, has highlighted the phenomena of inferior, superior mirages, and rainbow [5]. Apart from the Halo phenomenon observed on May 9, 2019 in N'Djamena, the Chadian National Meteorological Agency (ANAM) has given no explanation for the other optical phenomena observed in the Chadian atmosphere. It can be used to forecast short-term weather variations.

What's more, little attention is paid to the optical phenomena observed in Chad's atmosphere. Apart from a few optical phenomena observed in Chad, weather forecasts rarely mention these phenomena.

Unlike Madagascar, an island with a humid tropical climate, the question arises as to whether such phenomena can be observed in Chad's atmosphere. In order to answer this question, we simulated the refractive index of several regions of Chad with tropical, Sahelian and desert climates. The present work, which is a contribution to the study of optical phenomena observed in the Chadian atmosphere, will be structured as follows: Section 2 presents the methodology and some of the equipment used. In Section 3, the results of refractive index simulations for the selected cities will be presented, in order to find out whether it is likely to observe those optical phenomena such as mirages, rainbow and halo, observed by refractive index simulations of the Malagasy continent [5]. In Section 4, we will discuss these results and compare them with those found in the literature. We will then conclude our work.

2. Materials and Methodology

2.1. Materials Used

For this study, we used data from the Chadian National Meteorological Agency (ANAM), the Agency for Air Navigation Safety in Africa and Madagascar (ASECNA), and data from the Atmosphere, Climate and Environment Physics Laboratory (LAPACE) of the Faculty of Exact and Applied Sciences of the University of Ndjamena, from 1991 to 2020. Finally, Excel software was used to simulate the variation in optical refractive index for the different cities selected.

Table 1. Average temperature, rainfall and sunshine in the town of Faya-Largeau.

Months	Average Température (˚C)	rainfall (mm)	Corresponding days	Daily sunshine (hours)	Monthly sunshine (hours)
January	20	0	0	10	305
February	22	0	0	10.5	290
March	26	0	0	10	305
April	30.5	0	0	10.5	310
May	33	1	0	11	345
June	34	2	0	11	335
Juily	33.5	3	1	11	335
August	33	11	1	10.5	320
September	33	1	0	10.5	310
October	30	0	0	10.5	320
November	24.5	0	0	10.5	310
December	21	0	0	10	305
Year	28.3	18	2	10.4	3790

Table 2. Average temperature, rainfall and sunshine in Abeche.

Months	Average Température (˚C)	rainfall (mm)	Corresponding days	Daily sunshine (hours)	Monthly sunshine (hours)
January	26.3	0	0	12.5	305
February	27.9	0	0	13	290
March	31.4	0	0	14.2	305
April	32.9	25.9	0	14.2	310
May	33. 8	195. 8	0	18.2	345
June	33.7	65.2	0	11	335
July	30.36	284	1	10	335
August	28.1	76	1	11	320
September	29.45	59.2	0	12.3	310
October	30.69	0	0	13.6	320
November	28.39	0	0	14	310
December	25.03	0	0	13.2	305
Year	29. 85	706.1	2	10.4	3790

Table 3. Average temperature, rainfall and sunshine in Mongo.

Months	Average Température (˚C)	rainfall (mm)	Corresponding days	Daily sunshine (hours)	Monthly sunshine (hours)
January	26.97	0	0	9.25	105
February	28.48	0	0	10.5	210
March	32.65	0	0	13	225
April	34.4	10.32	0	15	235
May	30.9	32.25	0	10	215
June	31.01	73.23	0	13	225
July	26.86	170.25	1	8	100
August	25.51	255.78	1	9	102
September	27.52	100.21	0	9	102
October	29.42	25.36	0	10.3	210
November	29.11	0	0	10.3	310
December	25.71	0	0	10	210
Year	28. 83	643.73	2	10.1	2363

Table 4. Average temperature, rainfall and sunshine in Moundou.

Months	Average Température (˚C)	rainfall (mm)	Corresponding days	Daily sunshine (hours)	Monthly sunshine (hours)
January	25.5	0	0	9	280

Continued

February	28.8	0	1	9	250
March	31.6	5	2	8	250
April	32.2	40	5	8	235
May	29. 8	90	9	8	240
June	27.3	150	12	7	210
July	26.3	260	15	6	185
August	25. 8	285	19	5.5	170
September	25.2	200	13	6	185
October	27.5	55	7	7.5	235
November	27.1	2	2	9.5	380
December	25.3	0	0	9.5	290
Year	27.7	1085	85	7.7	2810

Table 5. Average temperature, rainfall and sunshine in Ndjamena.

Months	Average Temperature (˚C)	rainfall (mm)	Corresponding days	Daily sunshine (hours)	Monthly sunshine (hours)
January	23.7	0	0	9.5	300
February	27.1	0	0	10	275
March	31.2	0	1	9	280
April	34	10	3	9	275
May	33. 8	25	6	9	285
June	31. 8	50	9	8.5	260
July	28. 8	145	13	7	215
August	27.1	175	15	6.5	200
September	28.5	85	9	7.5	230
October	30	20	3	9	285
November	28	0	21	10	300
December	24.6	0	0	10	305
Year	29	510	60	8.5	3205

Finally, we used Excel to plot histograms of refractive index variation for the Faya-Largeau, Abeche, Mongo, Moundou and N'Djamena stations.

2.2. Methodology

The refractive index is given by the following empirical formula:

$$n = 1 + (ns - 1) \times \left(\frac{P(h)}{P_o}\right) \times \left(\frac{To}{T_{moy}}\right), \quad (1)$$

ns: the refractive index of the ground with a value of 1.00027697;

P_0: the pressure prevailing at station level brought down to sea level with a value of 1013.25 hPa;

(h): the pressure prevailing at station level;

T_{moy}: the average monthly temperature of a station;

T_0: the absolute temperature in kelvin.

The refractive index of the Earth's atmosphere depends essentially on the following two parameters:

- atmospheric pressure P in Pascal (Pa),
- atmospheric temperature T in Kelvin (K).

Knowing the height of the station and the average temperature, the absolute temperature is given by:

$$T_0 = T_{moy} + 6.5h\ station \tag{2}$$

T_{moy}: Average station temperature given by the relationship:

$$T_{moy} = \frac{T_{\max} + T_{\min}}{2} \tag{3}$$

h station represents the altitude of the station where the weather balloon used to record meteorological data was launched.

Furthermore, air temperature and pressure vary continuously with altitude according to the empirical relationship below:

$$P(h) = P_O \left(\frac{288 - 0.0065h}{288} \right)^{5.255} \tag{4}$$

In order to highlight the phenomenon of mirages, the refractive index of the atmosphere was calculated for five (5) cities in Chad, namely Faya-Largeau, which has a desert climate, Abeche, Mongo, N'Djamena, which has a Sahelian climate, and finally the region of Moundou, which has a tropical climate.

For our numerical simulations, the height h is taken to be 50 metres, giving a pressure $P(h)$ = 1006.87 hPa. As for temperatures, we have taken monthly averages over the 30 years of record from 1991 to 2020. In Excel, the months are entered on the x-axis and the corresponding refractive indices are calculated and plotted on the y-axis. This enabled us to obtain diagrams of monthly variations in refractive index.

3. Results

1) In Faya-Largeau city

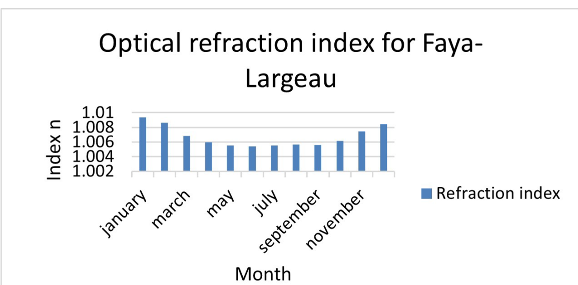

Figure 1. Variation in the refractive index of Faya-Largeau city from 1991 to 2020.

2) In Abeche city

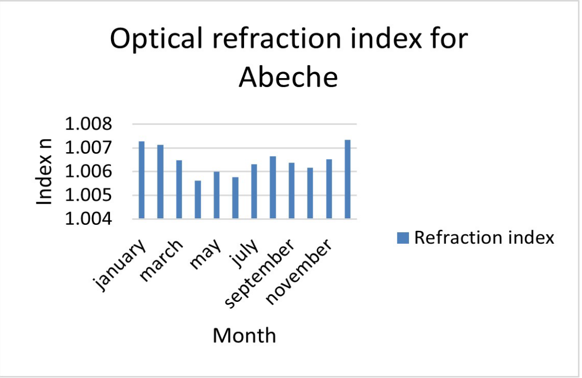

Figure 2. Variation in the refractive index of Abeche city from 1991 to 2020.

3) In Mongo city

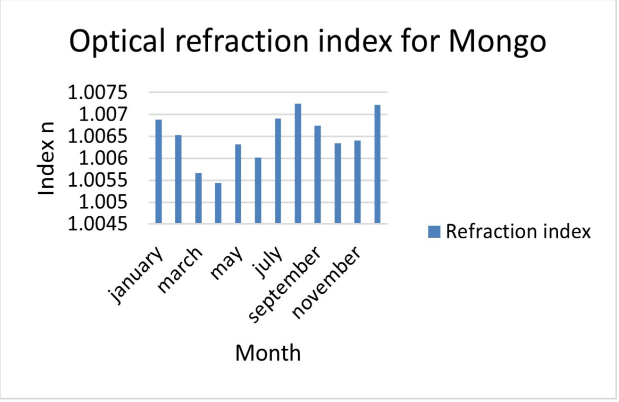

Figure 3. Variation in Mongo city's refractive index from 1991 to 2020.

4) In Moundou city

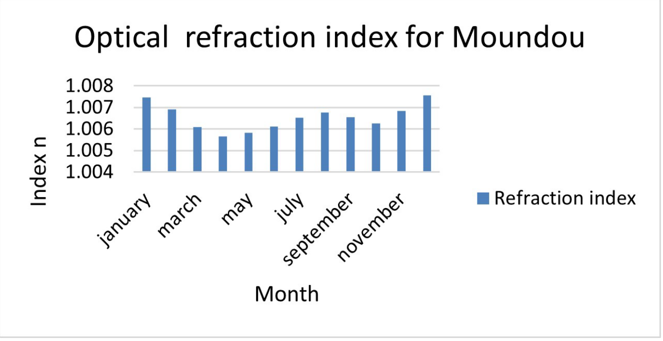

Figure 4. Variation in the refractive index of Moundou city from 1991 to 2020.

5) In N'Djamena city

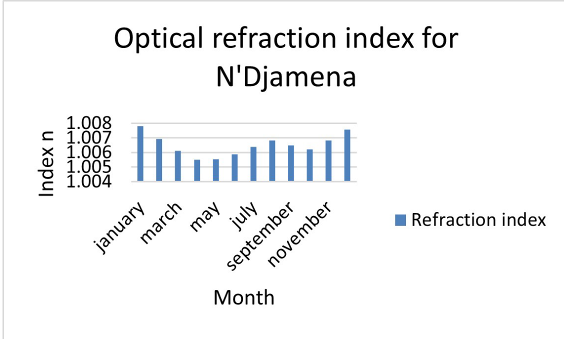

Figure 5. Variation in the refractive index of N'Djamena city from 1991 to 2020.

For the days of 02 July and 27 August 2021 at Hassan Djamous airport in N'Djamena city at 12 noon, the data enabled us to obtain an aerological diagram using Messir-Saddis software.

Figure 6. Image of a halo of light observed in N'Djamena city on May 9, 2019 (source ANAM).

4. Discussion

The city of Faya-Largeau is characterized by a desert climate. Table 1 shows that the highest average temperature is 34˚C. Rainfall is very rare and the sun shines throughout the year, with an average of 3,790 hours of sunshine per year (Table 1). It is one of the sunniest regions in Chad.

We can see in Figure 1 that, from January to June, the temperature gradually increases, causing a decrease in the refractive index during the propagation of light. As a result, light rays are bent upward, and the image of any object in the propagation space is located below the object, allowing us to observe the phenomenon of inferior mirage. However, from June to July, the refractive index increases slightly, remains fairly constant from July to September, and increases again from September to December. The temperature decreases and the refractive index increases. During propagation, light rays are bent downward and the image of the object is located above the real object. The superior mirage can be observed from June to July, then from September to December. However, during the period from July to September, when the refractive index is constant, neither the superior mirage nor the inferior mirage can be observed. The inferior mirage that can be observed from January to June is very similar to that observed in [13], because although our methodological approach is different, our simulated refractive indices at low altitudes vary around the value n = 1.0025, as is the case in [13]. Given the significant temperature inversion from January to June, a wide band of inferior mirage can be observed compared to those observed in studies [13] and [14]. However, the superior mirage that could be observed from June to July and from September to December will be of low amplitude [10] and [11] compared to the inferior mirage that could be observed in this region. The interval from July to September, when the refractive index remains constant, corresponds to the minimum distance between the observer and the ground, below which neither the object nor its image can be observed [14].

Although the sun shines every month of the year, the absence of precipitation does not favor rainbow formation, making it virtually impossible to observe rainbows in this part of the country.

In Abeche city, the data in **Table 2** show that the highest average temperature is reached in May, with a monthly average of 33.8˚C. The amount of precipitation is 706 mm per year. In this city, rainbows can be seen when it rains and the sun is shining. **Figure 2** shows that the refractive index is highest in December and January and then reaches its lowest value in April, so the refraction of sunlight on a surface or any object can lead to the observation of a succession of inferior and superior mirages. From January to April, there is a decrease in the refractive index, which may give rise to the observation of the inferior mirage phenomenon. This same phenomenon is observed on a curve from May to June, and is moderately observed from August to October. On the other hand, the superior mirage phenomenon is observed for a short period from April to May, and moderately observed from June to August, and from October to December. Since light rays propagate through air, the refractive index varies between 1.0045 and 1.0075, closer to the optical index of air, which is 1.00025 in [13]. This slight difference is due to the height of our station, which is 50 m above the ground. At an average altitude of 800 m in the troposphere, the variation in our refractive indices corroborates those in studies [5] and [15], which show an increase in the regions where inferior mirages are observed, but a decrease in the amplitude of the region where it is likely to observe the superior mirage phenomenon studied in the works [5] and [10]. The presence of average precipitation and abundant sunshine observed in **Table 2**, makes it possible for light to refract and reflect off raindrops, giving rise to the observation of rainbows.

In Mongo city, the average temperature of the hottest month is 34.4˚C in April and that of the coldest month is 25.51˚C in August. The annual rainfall total is 643.73 mm per year. The refraction of light on raindrops can cause rainbows to form. **Figure 3** shows that the refractive index is highest in August and lowest in April. Thus, the phenomenon of inferior mirages can be observed over a long period from January to April, over an average period from August to October, and finally over a short period from May to June.

However, in December, and finally from June to August, it can be observed over a fairly long period. The period from October to November, when there is virtually no variation in the refractive index of light, does not allow for the observation of mirages. This invariance of the refractive index corresponds to the minimum distance between the observer and the object, below which neither the object nor its image can be observed [16]. The presence of average precipitation and strong sunshine observed in **Table 3** would result in rainbows being observed when the sun shines on its horizon after rain in this region.

In Moundou city, the climate is tropical with a dry season from November to April and a rainy season from May to October. The data in **Table 4** show that the hottest period is from February to April before the rains, the average temperature of the coldest month (September) is 25.2˚C, and that of the hottest month is 32.2˚C in April.

The annual total precipitation is 1085 mm (**Table 4**). Sunshine during the dry season decreases more in the rest of the country, with an average of 2810 hours per year (**Table 4**).

The refractive index is highest in January and December and lowest in April (**Figure 4**).

As it rains heavily, the refraction and reflection of sunlight on raindrops can give rise to the observation of rainbow phenomena. **Figure 4** shows that from January to April, the refractive index decreases and the temperature increases. The same phenomenon is observed from August to October, with light rays bending upward in perfect accordance with the laws of geometric optics, according to which refracted rays deviate from the normal when the optical system passes from the most refractive medium to the least refractive medium. The image of the object is perceived below the actual object, so we observe the inferior mirage over a long period from January to April, and then over a short period from August to October. However, from May to August and from October to December, the temperature decreases and the refractive index increases. We observe the opposite phenomenon, with the curvature of the propagating light rays turned downward, so the image of an object will be perceived above the actual object, which is the domain of observation of the superior mirage.

In N'Djamena city, the annual rainfall total is 510 mm, with the first rains occurring in May and the last in early November (**Table 5**).

The annual temperature of the coldest month is 23.7˚C in January, and that of the hottest month is 34˚C in April (see **Table 5**).

The sun shines regularly during the dry season, while during the rainy season, the hours of sunshine decrease slightly. The least sunny month is August, with an average of 3205 hours of sunshine per year.

In **Figure 5**, we can see that the refractive index reaches its maximum in January and its minimum in April. From January to April, the refractive index decreases, and we observe inferior mirages. Then, from May to August, the refractive index increases, and we observe superior mirages. From August to October, the refractive index decreases and then increases again until December.

In references [13] and [15], the authors showed the possibility of locating a lower mirage by simulating the optical refractive index, as an exponential function of the y quadrature, and amplitudes or constants α and β dependent on the temperature profile. Using a similar approach to the two works above, Cruzado *et al.* [14] by studying the conditions of appearance of the inferior mirage, show the possibility of observing the object and its image in a certain region of the given space. By studying the inversion of the temperature profile, Lehn [14] shows that one can, under certain conditions, observe the phenomenon of superior mirage.

Our results, although statistical, but obtained thanks to average values of physical parameters taken over thirty (30) consecutive years, give with less margins of error, the possibility of observing the superior and inferior mirages studied in this manuscript.

Under these weather conditions, optical phenomena such as rainbows, mirages, and halos around the sun can be observed if the sky is dotted with cirrus and cirrostratus clouds. In addition to the mirages and rainbows highlighted by numerical simulations, on May 9, 2019, at Hassan Djamous Airport in N'Djamena, the observed halo phenomenon is shown in **Figure 6**. According to the theory of halo classification, the halo observed in Chad belongs to the family of halos known as small halos [16], which take the form of a point of light caused by the interaction between ice crystals and a ray of light propagating in the atmosphere. This small halo, also known as a 22˚ halo, is formed by the interaction of cirrus clouds with ice crystals in a cold or low-altitude atmosphere. Observed at low altitudes, *i.e.* below 800 meters, this small, point-shaped halo has a lifetime that can vary from a few seconds to tens of minutes. Generally speaking, the lifetime of a halo depends on the meteorological conditions in the space where it forms.

5. Conclusion

In this manuscript, we simulated the variation in the refractive index of the atmosphere, which is a function of pressure and temperature. Based on meteorological data available from institutions such as ASECNA, ANAM, and the Laboratory of Atmospheric, Climate, and Environmental Physics (LAPACE), we plotted histograms showing the annual variation in the refractive index for several cities in Chad. Apart from the city of Faya-Largeau, which has a desert climate, where we observed through simulation the phenomenon of inferior mirages from January to June and superior mirages from June to December, the three cities of N'Djamena, Mongo, and Abeche, which have a Sahelian climate, exhibit a succession of inferior and superior mirages of low amplitude in the same year compared to those observed in Faya-Largeau in the desert climate. However, in Moundou, with its tropical climate, a wide range of inferior and superior mirages is observed from January to August, followed by a narrow range of the same mirages from August to December. Studies conducted by Abraham Michaella Nomena in 2016 [5] show that the refractive index of the Earth's atmosphere is close to 1, which is in perfect agreement with our results reported in this manuscript.

Conflicts of Interest

The authors declare no conflicts of interest regarding the publication of this paper.

References

[1] Megle, G. (1993) Atomes et Atmosphère. *Mémoires de la Société Géologique de France*, **162**, 229-236.

[2] Taillet, R. (2006) Optique Physique, propagation de la lumière. Librairie Eyrolles.

[3] Benson, H. (2005) Physique 3: Ondes, Optique et Physique modern. De Boeck SUP.

[4] Aurélien, B. Réfraction et dispersion atmosphérique, Chapitre 3.

[5] Nomena, A.M. (2015) Etude de l'indice de réfraction de l'Atmosphère à Madagascar. Ph.D. Thesis, Université d'Antananarivo.

[6] Dettwiller, L. (2023) Phénomènes de réfraction atmosphérique terrestre. *Comptes Rendus. Physique*, **23**, 103-132. https://doi.org/10.5802/crphys.114

[7] Lehn, W.H., Silvester, W.K. and Fraser, D.M. (1994) Mirages with Atmospheric Gravity Waves. *Applied Optics*, **33**, 4639-4643. https://doi.org/10.1364/ao.33.004639

[8] Young, A.T. (2023) Did Monge Really Explain Inferior Mirages? *Comptes Rendus. Physique*, **23**, 467-481. https://doi.org/10.5802/crphys.106

[9] van der Werf, S.Y. (2011) Noninverted Images in Inferior Mirages. *Applied Optics*, **50**, F12. https://doi.org/10.1364/ao.50.000f12

[10] Lehn, W.H. (1983) Inversion of Superior Mirage Data to Compute Temperature Profiles. *Journal of the Optical Society of America*, **73**, 1622-1625. https://doi.org/10.1364/josa.73.001622

[11] Dettwiller, L. (2019) Some Theorems on "Arctic Mirages": Hillingar Effect and Superior Mirages. *Journal of the Optical Society of America A*, **36**, 1997-2004. https://doi.org/10.1364/josaa.36.001997

[12] Trucker, R.A.R. (1979) Ice Crystal Haloes. Atmospheric Optics Technical Group of the Optical Society of America.

[13] Alejandro Paola, C., Cruzado, A. and Carrasco Galleguillos, F.M. (2022) Light Refraction in the Earth's Atmosphere I. Inferior Mirages: Analytic Solution of Ray Paths. *Revista Mexicana de Física*, **68**, Article ID: 041301. https://doi.org/10.31349/revmexfis.68.041301

[14] Cruzado, A., Cesanelli, A. and Alejandro Paola, C. (2023) Light Refraction in the Earth's Atmosphere II. Inferior Mirages: Regions for Images and Objects Observation. *Revista Mexicana de Física*, **69**, Article ID: 061303. https://doi.org/10.31349/revmexfis.69.061303

[15] Cruzado, A., Alejandro Paola, C. and Cesanelli, A. (2024) Light Refraction in the Earth's Atmosphere III. Inferior Mirages: Images Locus. *Revista Mexicana de Física*, **70**, Article ID: 031301. https://doi.org/10.31349/revmexfis.70.031301

[16] Dettwiller, L. (2005) Classification des phénomènes de Halos, résultats analytiques et découvertes récentes. *Bull. Un. Phys.*, **99**, 877-878.